Aligned carbon nanotubes

Desktop Growth of Carbon-Nanotube Monoliths with In Situ Optical Imaging**

Anastasios John Hart, Lucas van Laake, and Alexander H. Slocum*

Driven largely by application-oriented interest in the exceptional electrical, mechanical, and thermal properties of carbon nanotubes (CNTs),[1] the process of catalytic chemical vapor deposition (CVD) has been developed for synthesis of CNTs in a wide variety of configurations. For example, isolated CNTs are grown on substrates for use as high-performance field-effect transistors,[2] aligned "forests" of CNTs are fabricated for use as thermal interface materials,[3] and floating catalyst processes enable the gas-phase CVD synthesis of CNTs in bulk quantities for applications in rechargeable batteries and electrically conductive plastics.[4, 5]

Laboratory-scale CVD synthesis methods typically use small tube furnaces, where the catalyst sample is placed within a sealed reaction tube, which is filled with the reactant mixture (e.g., a hydrocarbon or alcohol vapor). Tube furnaces are ubiquitous and easy-to-use systems; however, the large thermal mass of a tube furnace limits heating and cooling rates to typically no faster than $1\,^{\circ}\mathrm{C\,s^{-1}}$, and the enclosed heater geometry makes it difficult to observe the reaction in situ. Further, because the tube and substrate are held at the same temperature, the reactant mixture is prone to thermally induced decomposition as it flows through the tube and toward and over the substrate. This inherent coupling between the "activity" of the reactant and the temperature of the furnace prevents much further understanding of the relationship between the chemistry of the reactant precursor and the mechanism of CNT growth. In a laboratory tube furnace this typically causes the yield and quality (e.g., film thickness, alignment, graphitic quality) of CNTs to be sensitive to the placement of the growth substrate within an isothermal region of the furnace.[6] A previous investigation

[*] Dr. A. J. Hart, L. van Laake, Prof. A. H. Slocum
Department of Mechanical Engineering
Massachusetts Institute of Technology
77 Massachusetts Avenue, Room 3-470
Cambridge, MA 02139 (USA)
Fax: (+1) 617-258-6427
E-mail: ajhart@mit.edu

Supporting information for this article is available on the WWW under http://www.small-journal.com or from the author.

of these coupled effects used a high-velocity jet impinging upon a heated growth substrate at low pressure, in order to prevent homogeneous gas-phase reactions from occurring before the reactant reached the substrate. This demonstrated that pure acetylene reacting on the surface of Fe catalyst can grow a film of vertically aligned single-walled CNTs.[7]

Here, we utilize a custom-built desktop reactor apparatus[8] for synthesis of "monolithic" forests of aligned CNTs, where the reaction takes place in open view locally on a suspended silicon platform that is heated resistively (Figure 1). The small thermal mass of the substrate enables rapid heating and cooling ($\approx 100\,^{\circ}\mathrm{C\,s^{-1}}$) at relatively low power. Dedicated rapid thermal pretreatment of the reactant mixture at a temperature exceeding the substrate temperature is enabled by optionally first passing the gas through a heated Al_2O_3 pipe, which is fitted to the inlet of the tube end cap. Digital imaging of the substrate during the reaction reveals the film thickness versus time, and shows how film topography evolves due to spatial nonuniformities in the growth rate. Previous approaches to thermally localized growth of CNTs involve resistive heating of microfabricated traces and bridges,[9, 10] of silicon on a stage,[11–13] of a wire,[14] of carbon cloth coated with catalyst,[15–17] and generally of "hot-plate" stages as in plasma-enhanced CVD.[18] Our suspended platform configuration is scalable to large-area production of aligned CNTs by a continuous feed, and dedicated gas pretreatment and optical monitoring offer new opportunities for reaction diagnostics and manufacturing process control.

For growth of CNTs, a silicon substrate coated with a catalyst film of Fe/Al_2O_3 is placed at the center of the heated platform, and the platform is heated to 810 °C within 5 s of applying power. The temperature is maintained using a constant supply current. After heating, the substrate is first treated for 2 min in a reducing ambient to cause the film to coarsen into nanoparticles, and then the reactant mixture containing C_2H_4 is introduced for the desired growth time. In the initial work presented here, we only utilize the rapid heating and cooling capability to reduce the cycle time for our experiments from approximately 60 min to less than 30 min. A "cap" substrate is rested on top of the growth substrate; the cap moderates the reactant supply to the growth substrate and serves as an optical reference. The CNT film lifts the cap as it grows.[6, 19] Further process details are given in the Experimental Section.

CNTs grow from the catalyst-coated substrate, adopting the well-known vertically aligned CNT (VA-CNT) "forest" conformation, where the CNTs initially crowd and self-align while growing perpendicular to the substrate.[20] Using a reactant mixture of $C_2H_4/H_2/Ar$, which is delivered directly from the gas tanks, the CNT film grows to ≈ 0.1 mm thickness in 15 min (average growth rate of $7\,\mu\mathrm{m\,min^{-1}}$) at a platform temperature of 810 °C. At the same platform temperature, when the gas is first thermally pretreated by flowing it through the heated pipe, the film grows to be a monolith of 1.5 mm thickness in 15 min (average growth rate of $100\,\mu\mathrm{m\,min^{-1}}$). In an identical experiment using $C_2H_4/H_2/CO$, the film thickness exceeds 2.0 mm after 15 min and some areas reach nearly 4 mm after 45 min (Figure 2). Scan-
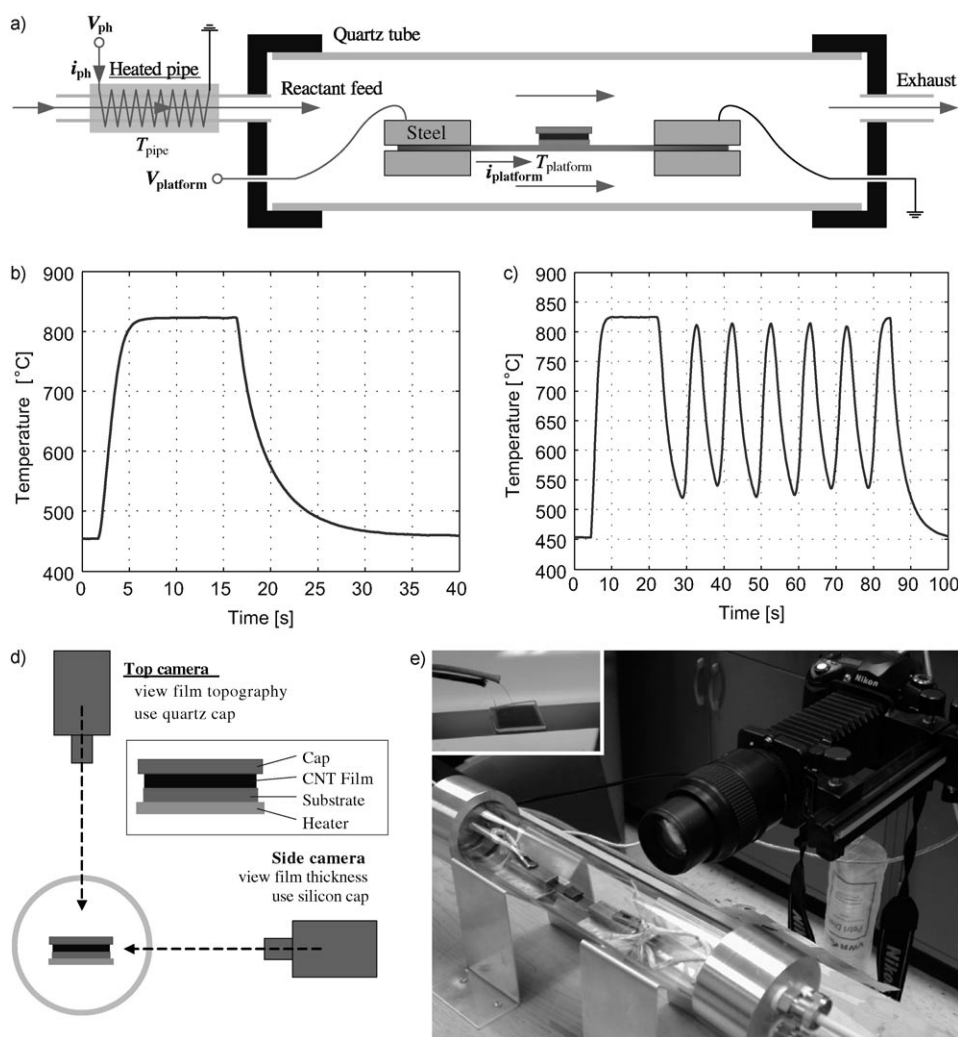
Figure 1. Desktop reactor apparatus for CNT film growth on a suspended resistively heated silicon platform:[8] a) Schematic of substrate in sealed quartz tube with heated pipe for optional thermal pretreatment of reaction gases; b) rapid heating of platform to 825 °C using step current and subsequent rapid cooling by discontinuing power; c) rapid cycling of platform temperature by oscillating supply current; d) configuration for in situ optical imaging of growth from top and side; e) laboratory setup with digital-still-camera imaging from side (inset image of platform with thermocouple affixed to underside).

cap is tilted upward to the right in the images; this tilt increases with continuing growth. Overall, we observe that these nonuniformities in growth rate are typical for films that grow rapidly, and emerge as growth slows in some regions of the film (likely due to decreasing activity of the catalyst) while growth remains more rapid in other regions.

Imaging of growth from the top view (Figure 4) concurrently shows that growth begins within the first imaging interval; after 15 s, a contrast band appears at the left of the image, corresponding to the edge of the catalyst film. Within the first 5 min, white spots appear in the images, corresponding to pits in the film where the growth rate is relatively slow. Formation and propagation of cracks (splits) in the film is also visible; for example, at $t = 570$ s in this experiment, a wall of VA-CNTs breaks away at the right edge of the substrate (Figure 4d) and grows away from the remainder of the film. A broad crack is also visible across the bottom of the image at $t = 570$ s, and at $t = 840$ s, another large crack initiates here and cuts across the middle area of the film as

ning electron microscopy (SEM) imaging of the film sidewalls reveals the alignment among the CNTs, and high-resolution transmission electron microscopy (HRTEM) imaging reveals that the CNTs are multi-walled with a diameter of 14.0 ± 4.8 nm (Figure 2b). By further SEM imaging, the density and alignment of the forest appear similar between the cases with and without thermal pretreatment, and with and without CO and Ar as carrier gases. Possible variations in the diameter distributions are under further investigation by TEM imaging; however, all these conditions give multi-walled nanotubes (MWNTs) having an average outer diameter of 10–20 nm.

Optical imaging of the heated platform from the side view (Figure 3) shows how VA-CNT film growth lifts the cap substrate, and upward displacement of the cap is visible starting within the first 15 s after introducing C_2H_4 to the chamber. Starting at $t \approx 10$ min, a significant nonuniformity in film thickness is apparent, as the reference edge of the

shown in the subsequent images. This technique confirms that cracks we observe in films grown in a tube furnace form during rather than after growth, further emphasizing the potential importance of mechanical stresses in mediating rapid growth of thick VA-CNT films. Comparison with a composite SEM image (Figure 2e) taken ex situ shows the significant microscale topographical features of a CNT film, which can be observed by this simple optical imaging technique. Videos (concatenated from still images) of growth viewed from the top and side are provided as Supporting Information.

Measuring the distance between the growth substrate and the cap, as shown on images taken during the growth reaction, directly reveals the film growth kinetics. This demonstrates that the film growth rate decreases slightly with increasing reaction time (Figure 5). Generally, VA-CNT growth can be limited by diffusion of the reactant through the film, or by the reaction rate at the catalyst. After the
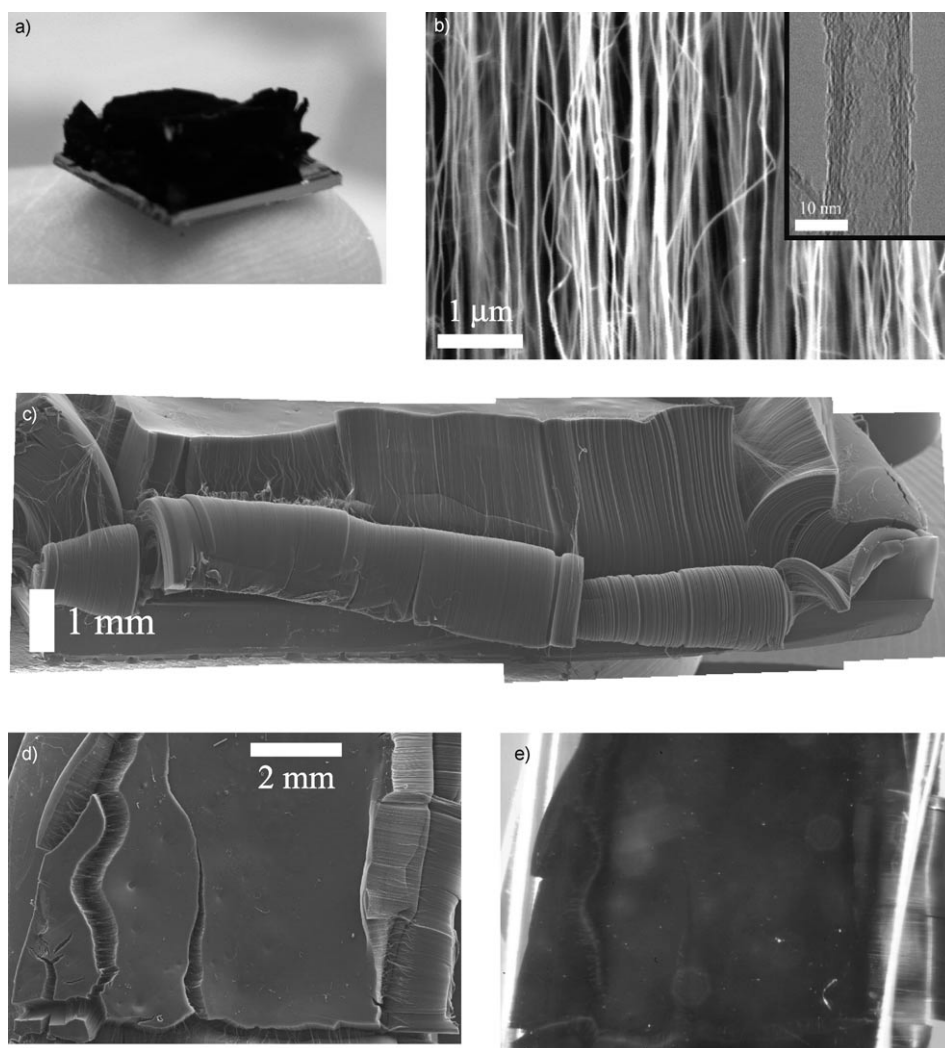
Figure 2. Monolithic VA-CNT films grown in $C_2H_4/H_2/CO$, on suspended reaction platform at 810 °C: a) Irregular monolith with ≈4-mm maximum height on silicon wafer substrate, resting on fingertip; b) alignment of CNTs within sidewall of a monolith, along with HRTEM image of an individual CNT taken from the monolith; c) composite SEM image of the sidewall of a monolith (same sample as in (d), (e), and Figure 4) showing areas that delaminated from the sidewall during growth; d) composite SEM image of the top surface of the monolith; e) top-view optical image of the monolith, taken in situ at the end of a growth sequence.

well-known Deal–Grove model for thermal oxidation of silicon,[21] as adopted for VA-CNT growth by Zhu et al.,[22] a diffusion-limited reaction progresses as

$$h = 0.5\sqrt{(A^2 + 4Bt)} - 0.5A \qquad (1)$$

The constants A and B can be related to the diffusion coefficient through the film and the reaction rate at the base of the film. Alternatively, Futaba et al.[23] suggest that growth is limited by a decaying reaction rate of the catalyst, where

$$h = \beta\tau_0\left(1 - e^{-t/t_0}\right) \qquad (2)$$

Here, β is the initial film growth rate, and τ_0 represents the catalyst lifetime. On one hand, the diffusion-limited model predicts that growth will slow gradually as it becomes more difficult for precursors to reach the catalyst at the bottom of the film, yet growth will never stop. Further, this model assumes perfect and constant efficiency of the catalyst, and neglects other critical aspects such as the polydispersity of the reactant mixture and diffusion of reaction products away from the catalyst. On the other hand, the decay-limited model neglects possible diffusion limitation, assuming there is always a sufficient supply of reactant to maintain the growth rate which is limited by the declining activity of the catalyst. Our initial data, limited to the first 15 min of growth due to the optical field of view, fits both models very well ($A = 4.51$, $B = 0.50$, $R^2 = 0.999$; $\beta = 0.11$, $\tau_0 = 29.75$, $R^2 = 0.999$). We observe that particular areas of the film suddenly stop growing after first slowing gradually, and therefore we believe that growth in our system is first diffusion-limited, and then growth is terminated by rapid deactivation of the catalyst. Nowadays, we are directly measuring the film thickness versus time using a laser displacement sensor, which is mounted above the heated platform. This ongoing work will be reported later as a detailed quantitative assessment of the limiting growth kinetics in our system.

The significant increase (≈1500%) in CNT growth rate when the reactant gas is thermally pretreated indicates that gas-phase decomposition of the reactants can significantly increase their activity for CNT growth, likely by forming species that are processed by the catalyst at a higher conversion rate. Further, because the gas cools after exiting the heated pipe, and then is reheated when it contacts the catalyst surface, new chemical species rather than radicals are contributing to this enhancement. The residence time of the gas in the heated pipe is ≈0.1 s, and forced convection flow calculations predict that the mixture heats to 1000 °C within this time.

The benefits of reactant preactivation in thermal CVD growth of CNTs have previously been realized by hot-filament methods, typically where the reactant flows over a
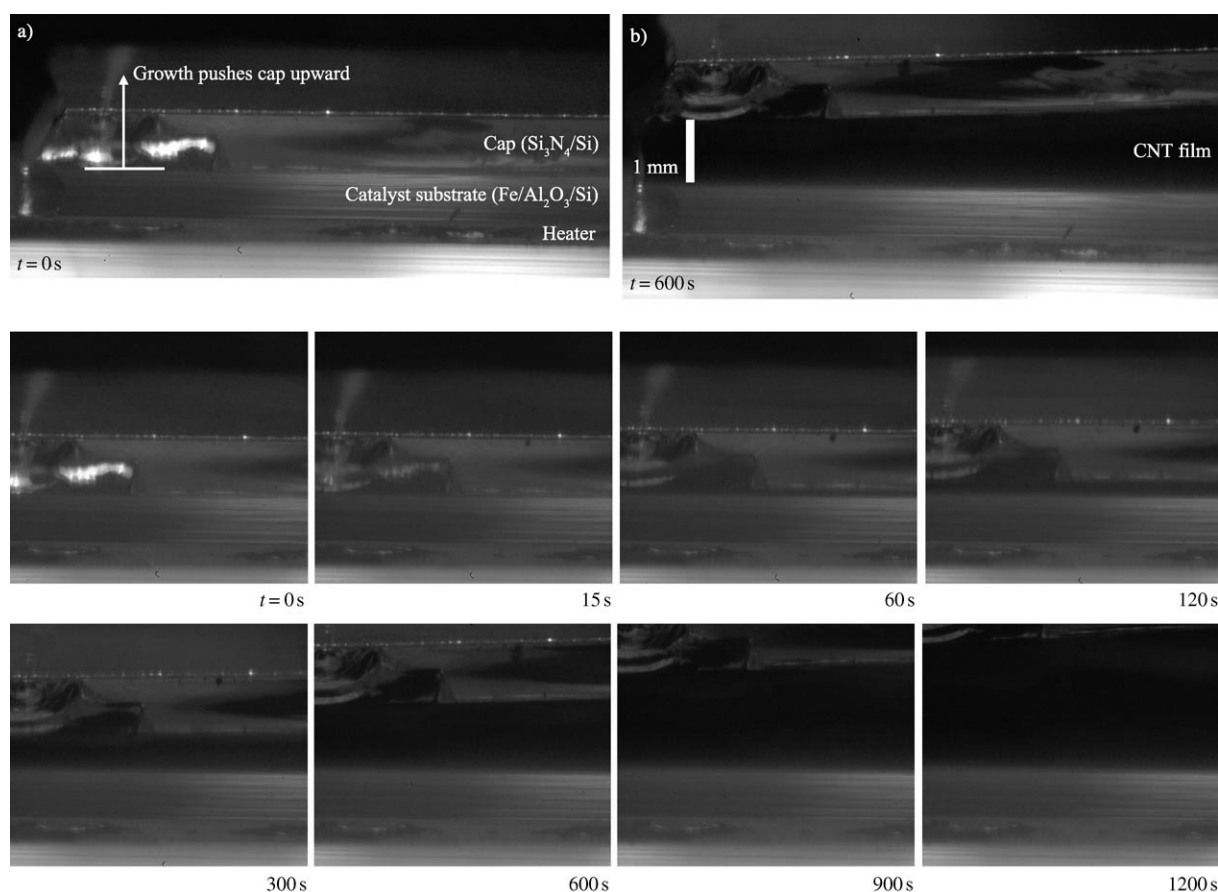
Figure 3. In situ side-view optical images of the thickness evolution of a VA-CNT film during growth on a resistively heated silicon platform mounted in a quartz tube, at a platform temperature of 810 °C. The film thickness is ≈ 2.0 mm after 20 min of growth.

wire that is resistively heated to over 1500 °C.[24–26] The wire is positioned upstream of the growth substrate or over the growth substrate, and in the latter case the filament can also heat the substrate. In our method, direct flow through a heated pipe ensures uniform activation of the gas, a short residence time ensures that significant sooting is avoided, and the preactivation temperature is fully decoupled from the growth temperature. Chemical simulation and analysis (e.g., mass spectrometry and gas chromatography) of the re-actant mixture before and after preactivation, and before and after growth, is ongoing and will help us understand which derivative products are more active, and are perhaps more suitable direct precursors for CNT nucleation and/or growth. Thermally induced decomposition of a hydrocarbon gives many stable and unstable products along with H_2; for example, C_2H_4 homogeneously reforms into C_2H_2, CH_4, C_2H_6, and many larger hydrocarbon molecules.[27] There are many reaction pathways between H_2 and C_2H_4, both in me-diating gas-phase pyrolysis of a hydrocarbon, and in medi-ating stability of graphitic fragments on transition metal sur-faces.[28–30]

Further, the additional increase in CNT growth rate when Ar is replaced with CO may occur because CO in-creases the conversion rate of C_2H_4 on Fe catalysts. It was reported previously that the addition of CO to C_2H_4/H_2 in-creases the yield of carbon filaments from Fe powder at 600 °C.[31] This is attributed to reorganization of the Fe sur-face to promote cleavage of the C=C bond in C_2H_4, and to enhanced formation of C_2H_6, which has more recently been used as a carbon source for high-yield CNT growth.[32] Fur-ther, CO has been widely used as a carbon source for CNT growth, such as for atmospheric-pressure growth of SWNTs from a Co/Mo catalyst at 800 °C,[33] and for elevated-pres-sure growth of SWNTs from Fe catalysts at 800–1200 °C.[34] We have only used CO as an additive, and have not evaluat-ed its efficacy as the primary carbon source for CNT growth in our system.

In conclusion, we have grown monolithic aligned carbon nanotubes (CNTs) to heights of multiple millimeters, using a desktop apparatus where the reaction temperature is lo-calized to a resistively heated silicon platform. By dedicated thermal pretreatment of a $C_2H_4/H_2/CO$ reaction mixture, CNTs are grown to 3-mm thickness in just 15 min at a plat-form temperature of 810 °C, using a catalyst film of Fe/ Al_2O_3 on Si, at atmospheric pressure. Full-view optical access to the platform facilitates in situ monitoring of the growth reaction, and optical imaging reveals the time evolu-tion of the CNT film thickness, along with cracking of the film due to spatial nonuniformities in growth rate and re-sulting mechanical stresses in the film. Control of the reac-tion temperature by resistive heating of a suspended sub-strate platform is scalable to continuous feed and large-area production of CNT films, and offers further opportunity for real-time reaction diagnostics.
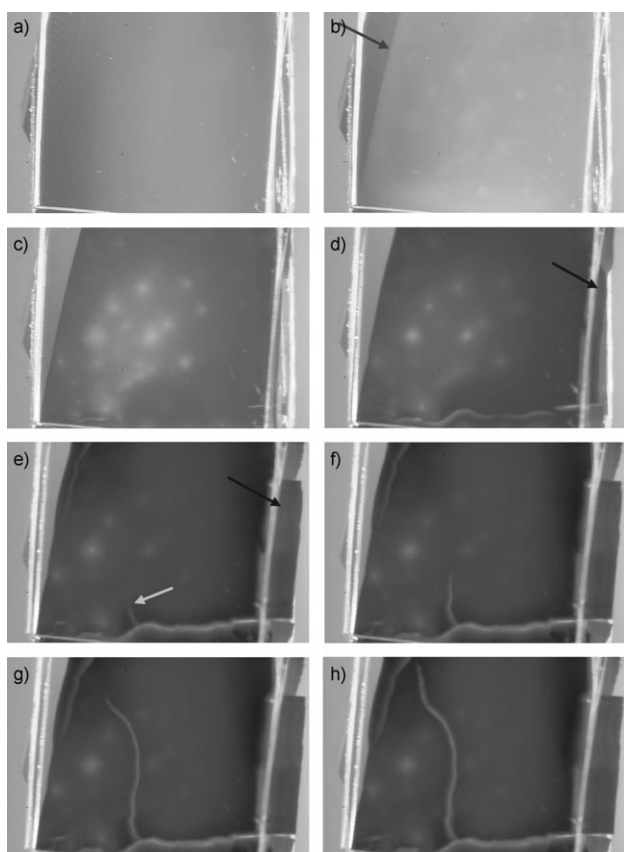
Figure 4. Top-view optical images of a $\approx 12 \times 12$ mm^2 area CNT film taken in situ during growth: a, b) Growth starts within the first 15 s of C$_2$H$_4$ supply, where the arrow indicates the edge of the catalyst film; c) pits develop in the film where the growth is slower, and these appear as bright spots in the optical image; d) an edge of the film (see arrow) breaks away due to stresses and grows to the right; e–h) the edge has grown considerably to the right, and a crack propagates through the interior of the film (lower arrow in (e)). Timescale: a) $t = 0$, b) 15 s, c) 300 s, d) 570 s, e) 840 s, f) 870 s, g) 900 s, h) 930 s.

Figure 5. Measurements of film thickness taken from side-view digital images shown in Figure 3, along with curve fits to diffusion-limited and decay-limited kinetic models.

Experimental Section

First, a catalyst film of 1/10 nm Fe/Al$_2$O$_3$ was deposited on a bare Si wafer by electron-beam evaporation, as described in our previous work.[6] A $\approx 1 \times 1$ cm^2 sample of the catalyst-coated substrate was placed on the suspended silicon platform heater, which was contained within a sealed quartz tube (300-mm length, 48-mm internal diameter (ID), 52-mm outer diameter (OD)), as shown schematically in Figure 1a. The platform was cleaved from a highly doped silicon wafer (300-μm thickness, 150-mm diameter, $N_A > 10^{18}$, Silicon Quest International). The suspended platform was clamped between stainless steel (AISI 304) blocks, and the blocks served as mechanical anchors and electrical contacts, and moved freely in response to thermal expansion. The platform temperature was calibrated using a 75-μm-diameter junction K-type thermocouple (Omega), which was affixed using ceramic adhesive (Ceramabond 865, Aremco) at the center of th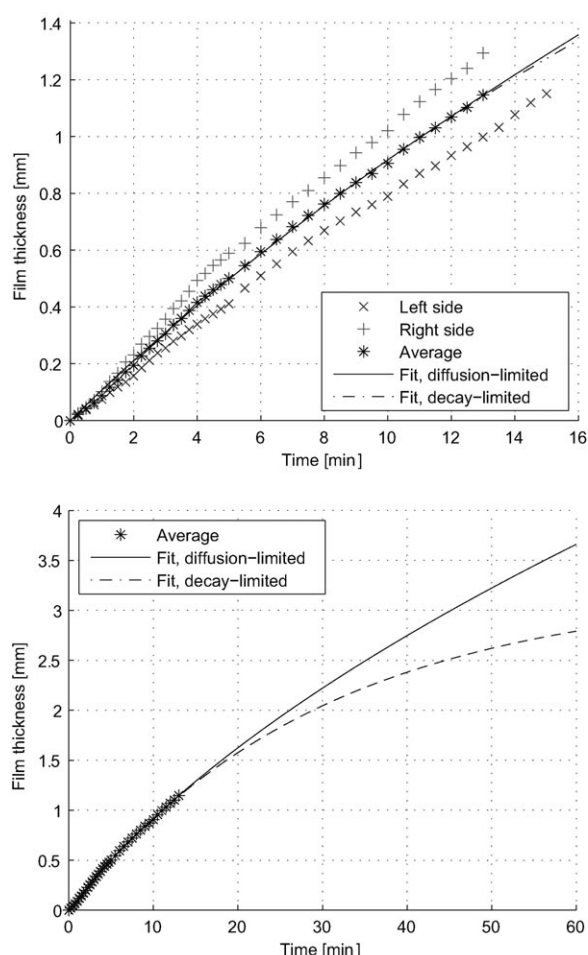e underside of the platform. The optical flatness of the polished platform surface ensured good thermal contact between the platform and the growth substrate, and therefore the temperature drop between the platform and the catalyst surface was less than 10 °C. The inlet to the quartz tube was fitted with a four-bore Al$_2$O$_3$ delivery pipe ("heated pipe", 6.35-mm OD, 1.8-mm bore ID, Vesuvius McDanel), which was heated by passing current through an iron wire wrapped tightly around the pipe ($R \approx 12 \ \Omega$ for 24 wraps around the pipe) and packed with insulation inside a firebrick enclosure.

For CNT growth, the tube was first flushed with 600 sccm Ar (99.999%, Airgas) for 10 min. After this, power was first delivered to the heated pipe (25 V under voltage control), and 3 min later the platform was heated (4.07 A under current control). The center area of the platform heated to 810 °C within 5 seconds. After 2 min, the flow was adjusted to 400/140 sccm H$_2$/Ar, and 5 min later the flow was adjusted to 115/400/100 sccm C$_2$H$_4$/H$_2$/Ar or C$_2$H$_4$/H$_2$/CO for the growth duration. The reactant gas penetrated the gap between the cap and the growth substrate and CNT growth lifted the cap. As we have studied previously, the weight of a single cap (≈ 0.2 g) is not sufficient to mechani-

cally suppress the growth rate or to alter the structure of the CNTs.[19]

During the reaction, the platform was imaged using a digital still camera (Nikon D150) with a zoom lens. The camera was mounted on a tripod and was oriented horizontally to view the growth progress from the side, or was oriented vertically to view the growth progress from the top. An image was taken every 15 s, starting 15 s before the reactant mixture was introduced to the tube.

The CNTs were characterized by scanning electron microscopy using a Philips XL30 operating at 5 keV, and by transmission electron microscopy using a JEOL-2011 operating at 200 keV. TEM samples were prepared by dispersing a section of the CNT monolith in 2-propanol with gentle sonication, and then placing two drops of the solution on a lacey carbon film (Ladd Research). Composite SEM images were digitally stitched using the Microsoft Research Image Stitcher.

Keywords:

[1] R. H. Baughman, A. A. Zakhidov, W. A. de Heer, *Science* **2002**, *297*, 787–792.
[2] A. Javey, J. Guo, Q. Wang, M. Lundstrom, H. Dai, *Nature* **2003**, *424*, 654–657.
[3] H. Huang, C. H. Liu, Y. Wu, S. S. Fan, *Adv. Mater.* **2005**, *17*, 1652–1656.
[4] M. Endo, *Chemtech* **1988**, *18*, 568–576.
[5] M. Endo, T. Hayashi, Y. A. Kim, H. Muramatsu, *Jpn. J. Appl. Phys. Part 1* **2006**, *45*, 4883–4892.
[6] A. J. Hart, A. H. Slocum, *J. Phys. Chem. B* **2006**, *110*, 8250–8257.
[7] G. Eres, A. A. Kinkhabwala, H. Cui, D. B. Geohegan, A. A. Puretkzy, D. H. Lowndes, *J. Phys. Chem. B* **2005**, *109*, 16684–16694.
[8] L. C. van Laake, A. J. Hart, A. H. Slocum, unpublished results
[9] O. Englander, D. Christensen, L. W. Lin, *Appl. Phys. Lett.* **2003**, *82*, 4797–4799.
[10] S. Dittmer, O. A. Nerushev, E. E. B. Campbell, *Appl. Phys. A* **2006**, *84*, 243–246.
[11] S. Chiashi, Y. Murakami, Y. Miyauchi, S. Maruyama, *Chem. Phys. Lett.* **2004**, *386*, 89–94.
[12] P. Finnie, J. Bardwell, I. Tsandev, M. Tomlinson, M. Beaulieu, J. Fraser, J. Lefebvre, *J. Vac. Sci. Technol. A* **2004**, *22*, 747–751.
[13] P. Finnie, A. Li-Pook-Than, J. Lefebvre, D. G. Austing, *Carbon* **2006**, *44*, 3199–3206.
[14] M. Croci, J. M. Bonard, O. Noury, T. Stockli, A. Chatelain, *Chem. Vap. Deposition* **2002**, *8*, 89–92.
[15] O. Smiljanic, T. Dellero, A. Serventi, G. Lebrun, B. L. Stansfield, J. P. Dodelet, M. Trudeau, S. Desilets, *Chem. Phys. Lett.* **2001**, *342*, 503–509.
[16] X. Sun, B. Stansfield, J. P. Dodelet, S. Desilets, *Chem. Phys. Lett.* **2002**, *363*, 415–421.
[17] X. Sun, R. Li, B. Stansfield, J. P. Dodelet, S. Desilets, *Chem. Phys. Lett.* **2004**, *394*, 266–270.
[18] K. B. K. Teo, D. B. Hash, R. G. Lacerdo, N. L. Rupesinghe, M. S. Bell, S. H. Dalal, D. Bose, T. R. Govindan, B. A. Cruden, M. Chhowalla, G. A. J. Amaratunga, M. Meyyappan, W. I. Milne, *Nano Lett.* **2004**, *4*, 921–926.
[19] A. J. Hart, A. H. Slocum, *Nano Lett.* **2006**, *6*, 1254–1260.
[20] S. S. Fan, M. G. Chapline, N. R. Franklin, T. W. Tombler, A. M. Cassell, H. J. Dai, *Science* **1999**, *283*, 512–514.
[21] B. E. Deal, A. S. Grove, *J. Appl. Phys.* **1965**, *36*, 3770–3778.
[22] L. Zhu, D. W. Hess, C.-P. Wong, *J. Phys. Chem. B* **2006**, *110*, 5445–5449.
[23] D. N. Futaba, K. Hata, T. Yamada, K. Mizuno, M. Yumura, S. Iijima, *Phys. Rev. Lett.* **2005**, *95*, 056104.
[24] S. Chaisitsak, A. Yamada, M. Konagai, *Diamond Relat. Mater.* **2004**, *13*, 438–444.
[25] Y. Ishikawa, H. Jinbo, *Jpn. J. Appl. Phys. Part 1* **2005**, *44*, L394–L397.
[26] N. Koizumi, Y. Minorikawa, H. Yakabe, H. Kimura, T. Kurosu, M. Iida, *Jpn. J. Appl. Phys. Part 1* **2006**, *4*, 6517–6523.
[27] G. D. Towell, J. J. Martin, *AIChE J.* **1961**, *7*, 693–698.
[28] Y. Nishiyama, Y. Tamai, *J. Catal.* **1976**, *45*, 1–5.
[29] N. Yoshida, N. Matsumoto, S. Kishimoto, *J. Catal.* **1985**, *92*, 177–179.
[30] G. A. Jablonski, F. W. Geurts, A. Sacco, R. R. Biederman, *Carbon* **1992**, *30*, 87–98.
[31] N. M. Rodriguez, M. S. Kim, R. T. K. Baker, *J. Catal.* **1993**, *144*, 93–108.
[32] G. Gulino, R. Vieira, J. Amadou, P. Nguyen, M. J. Ledoux, S. Galvagno, G. Centi, C. Pham-Huu, *Appl. Catal. A* **2005**, *279*, 89–97.
[33] B. Kitiyanan, W. E. Alvarez, J. H. Harwell, D. E. Resasco, *Chem. Phys. Lett.* **2000**, *317*, 497–503.
[34] P. Nikolaev, M. J. Bronikowski, R. K. Bradley, F. Rohmund, D. T. Colbert, K. A. Smith, R. E. Smalley, *Chem. Phys. Lett.* **1999**, *313*, 91–97.